Journal Pre-proof

Roles for heterodimerization of APJ and B2R in promoting cell proliferation via ERK1/2-eNOS signaling pathway

Bingyuan Ji, Liyan Shang, Chunmei Wang, Lei Wan, Baohua Cheng, Jing Chen
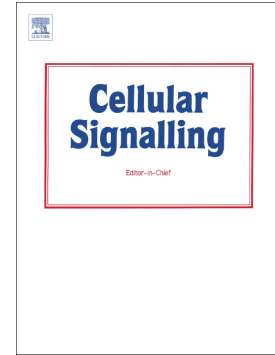
Please cite this article as: B. Ji, L. Shang, C. Wang, et al., Roles for heterodimerization of APJ and B2R in promoting cell proliferation via ERK1/2-eNOS signaling pathway, *Cellular Signalling* (2019), https://doi.org/10.1016/j.cellsig.2020.109671

Roles for heterodimerization of APJ and B2R in promoting cell proliferation via ERK1/2-eNOS signaling pathway

Bingyuan Ji[a,*] jby2006@mail.jnmc.edu.cn, Liyan Shang[b], Chunmei Wang[a], Lei Wan[a], Baohua Cheng[a], Jing Chen[a,c,*] Jing.Chen@warwick.ac.uk

[a]Institute of Neurobiology, School of Mental Health, Jining Medical University, Jining, 272067, P.R.of China

[b]Department of Nephrology, Zoucheng People's Hospital, Zoucheng, 273500, P.R.of China

[c]Division of Translational and Systems Medicine, Warwick Medical School, University of Warwick, Coventry, UK

[*]Corresponding authors.

Abstract

Apelin receptor (APJ) and bradykinin B2 receptor (B2R) play an important role in many physiological processes and share multiple similar characteristics in distribution and functions in the cardiovascular system. We first identified the endogenous expression of APJ and B2R in human umbilical vein endothelial cells (HUVECs) and their co-localization on human embryonic kidney (HEK) 293 cells membrane. A suite of bioluminescence and fluorescence resonance energy transfer (BRET and FRET), proximity ligation assay (PLA), and co-immunoprecipitation (Co-IP) was exploited to demonstrate formation of functional APJ and B2R heterodimer in HUVECs and transfected cells. Stimulation with apelin-13 and bradykinin (BK) increased the phosphorylation of the endothelial nitric oxide synthase (eNOS) in HUVECs, which could be inhibited by the silencing of APJ or B2R, indicating the APJ-B2R dimer is critical for eNOS phosphorylation in HUVECs. Furthermore, the increase of NOS and extracellular signal regulated kinases 1/2 (ERK1/2) phosphorylation mediated by APJ/B2R dimer can be inhibited by U0126 and U73122, respectively, suggesting that the heterodimer might activate the PLC/ERK1/2/eNOS signaling pathway, and finally leading to a significant increase in cell proliferation. Thus, we uncovered for the first time the existence of APJ-B2R heterodimer and provided a promising new target in cardiovascular therapeutics.

Keywords: APJ; B2R; eNOS; ERK1/2; Heterodimerization

Abbreviations

GPCR   G-protein-coupled receptor

APJ apelin receptor

B2R bradykinin B2 receptor

BK bradykinin

BRET   bioluminescence resonance energy transfer

FRET   fluorescence resonance energy transfer

PLA proximity ligation assay

eNOS   endothelial nitric oxide synthase

ERK1/2 extracellular signal regulated kinases 1/2

DAPI   4′,6-diamidino-2-phenylindole

PLC phospholipase C

Co-IP   co-immunoprecipitation

HUVEC   human umbilical vein endothelial cells

shRNA   short hairpin RNA
VSMC   vascular smooth muscle cell

1. Introduction

G-protein coupled receptors (GPCRs) constitute the largest family of cell surface receptors, and are essential components for the initiation of signal transduction from the outside to the inside of cells. Because they play crucial roles in the regulation of nearly every physiological process, GPCRs represent the targets for about 30% of globally marketed drugs [1, 2]. Although GPCRs were initially thought to perfectly function as monomeric entities, increasing evidence suggests that they can exist as dimers or oligomers which affect ligand binding, receptor traffic and signaling [3]. Numerous GPCRs have been shown to dimerize, and APJ or B2R are no exception [4, 5].

Apelin, a family of peptides derived from a 77-amino-acid prepropeptide, exert their physiological effects through binding to the apelin receptor (also known as APJ) [6], a member of the GPCR super-family. Apelin and APJ are widely distributed in the heart and vasculature, and play important roles in the physiology and pathophysiology of the cardiovascular system [7]. It has been demonstrated that apelin-13 possesses stronger activity compared to apelin-17 and apelin-36 [7]. Apelin usually binds to APJ and activates downstream Gαi/Gαo signaling, inhibiting cAMP production and inducing the phosphorylation of p42/44 ERKs [8]. Besides acting as a monomer, APJ heterodimerizes with other GPCR that regulate physiological function, including κ-opioid receptor (KOR) [9], angiotensin II type-1 receptor (AT1R) [10], neurotensin receptor 1 (NTSR1) [11], orexin receptor type 1 (OX1R) [12] and so on.

Bradykinin B2 receptor (B2R) and bradykinin B1 receptor (B1R) both belong to the family of GPCRs. In general, BK and kallidin bind to B2R which is constitutively expressed in a majority of healthy tissues, and particularly in endothelium and vascular smooth muscle cell (VSMC), while des-Arg^9-BK and des-Arg10-kallidin bind to B1R which is expressed under pathological conditions of tissue injury [13, 14]. Most of the physiological functions of kinins are mediated by B2R, and the major action of the B2R proceeds through Gαq subunit, resulting in PLC-mediated intracellular calcium mobilization. On the other hand, BK/B2R system could promote cell proliferation and vascular fibrosis through stimulating activation of ERK1/2 pathway [15, 16]. Likewise, the direct interaction between B2R and other GPCRs has been confirmed, causing changes in cell signaling and receptor functions. It has been demonstrated that B2R dimerize with TX-prostanoid receptors [5], dopamine D2 receptor (D2R) [17], AT1R and AT2R [18, 19], P2Y2 ATP receptors [20], as well as with KOR [21].

APJ and B2R share many congenerous characteristics. They are ubiquitously expressed in various cells of the cardiovascular system under both normal and diseased conditions where they exhibit similar functions in cardiovascular protection. For example, both receptors can promote angiogenesis by enhancing the expression of eNOS and vascular endothelial growth factor [22, 23]. In addition, Han et al. found that B2R promoted post-ischemic angiogenesis and cerebral perfusion after treated

with human urinary kallidinogenase through enhancing expression of apelin/APJ in ERK1/2 dependent way [24]. Finally, APJ and B2R could form functional dimers with different GPCRs. However, the likelihood of APJ-B2R heteromerization is not reported.

In this study, bioluminescence/fluorescence resonance energy transfer (BRET and FRET) microscopy, the proximity ligation assay (PLA) and co-immunoprecipitation (Co-IP) were used to measure the molecular proximity between APJ and B2R in HUVECs and transfected HEK293 cells, providing evidence for the quantification of receptor heterodimerization. Meanwhile, we examined whether the heterodimer changed the signal transduction of monomers, with particular interest in the phosphorylation of eNOS and ERK1/2, which play a critical role in the modulation of cardiovascular protection [25, 26]. Moreover, we demonstrated the effects of APJ-B2R dimers on cell activities.

2. Materials and methods

2.1. Plasmid constructs

The pcDNA3.1-APJ and pcDNA3.1-B2R plasmids were obtained from the UMR cDNA Resource Center (University of Missouri-Rolla, USA). Cyan fluorescent protein (CFP) or mVenus was attached to the C-terminus of APJ and B2R by inserting the open reading frame of APJ and B2R into the CFP-N1 or mVenus-N1 vector to create APJ-CFP and B2R-Venus. For the APJ-Rluc, the coding sequence of human APJ lacking a stop codon was subcloned into pRluc-N1 (BioSignal Packard, Inc., Montreal, Canada). To construct pEGFP-APJ, cDNA encoding human APJ was cloned into pEGFP-C1 (Clontech, USA). Other constructs presented herein were made using standard molecular biology as described previously [21]. All the resulting constructs were confirmed by commercial sequencing.

2.2. Cell culture and transfection

HUVECs and HEK293 cells were cultured in DMEM (GIBCO) with 10% fetal bovine serum (FBS) Sigma-Aldrich) at 37°C in a 5% CO_2 humidified incubator. To carry out transient transfection experiments, different plasmids were transfected into cells using Lipofectamine 2000 reagent according to the manufacturer's instructions. Membrane receptor expression was detected by reverse transcription-polymerase chain reaction (RT-PCR).

2.3. Immunostaining and confocal microscopy

HEK293 cells grown on coverslips were transiently transfected with pEGFP-APJ and pcDNA3.1-B2R and fixed after 24 h as previously described [21, 27]. Nonspecific binding was blocked by incubation with 3% bovine serum albumin prepared in PBS pH7.4 for 1 h at room temperature, and then permeabilized for 30 min with 0.01% Triton-X-100 in PBS. Cells were washed three times with PBS and incubated with an anti-B2R monoclonal antibody (1:200) in PBS at 4°C overnight. Cells were washed three times with PBS, followed by incubation with Alexa-Fluor®647 (red)-conjugated secondary antibodies (1:400) (Molecular Probes,

Invitrogen) for 1 h at room temperature. After a final wash with PBS, the cells were examined by Leica TCS SP8 scanning confocal microscope (Leica Microsystem, Germany).

2.4. Enzyme-linked immunosorbent assay(ELISA)

APJ and B2R expression in HEK293 cells was quantitatively assessed by ELISA [28]. The HA-APJ and Myc-B2R plasmids were alone or co-transfected into HEK293 cells. After 24 hours, HA-APJ, Myc-B2R, or HA-APJ/Myc-B2R cells were subcultured in 96-well microplates at a density of 2×10^5 cells per well. Cells were fixed with paraformaldehyde (4%) in PBS at room temperature for 30 min, and then washed three times with PBS. Next, cells were blocked in PBS containing 3% BSA, followed by incubating with primary mouse anti-Myc antibodies or rabbit anti-HA antibodies (Cell Signaling Technology) overnight at 4 °C. After washing three times with PBS, cells were incubated with goat anti-mouse or goat anti-rabbit horseradish peroxidase-conjugated secondary antibody for 1 h at 37 °C. After washing three times, the substrate 3,3′,5,5′-tetramethylbenzidine (200 μL) was added and incubated for 30 min at 37 °C, finally stopped with 50 μL of 0.2M H2SO4. The orange color reaction appeared only when the substrate reacted with the peroxidase enzyme conjugated to the secondary antibody, and the optical density was measured at 450 nm using an iMark Microplate reader (Bio-Rad , USA).

2.5. Bioluminescence resonance energy transfer (BRET) assays

HEK293 cells were transiently co-transfected with vectors encoding Rluc fusion or Venus fusion proteins. Twenty-four hours after transfection, cells were detached and transferred (10^5 cells/ well) to a 96-well microplate microplate white plates with an opaque bottom (Corning 3600, Stockholm, Sweden) in HEPES-buffered phenol red-free medium (Invitrogen, Life Technologies) for 24 h. Cells were then washed twice and resuspended in D-PBS (PBS containing 0.5 mM MgCl2 and 0.1% (w/v) glucose). Coelenterazine H substrate was used at final concentration of 5 μM. Analysis was made immediately using a Tristar LB941 plate reader (Berthold Technologies, Germany). The BRET ratio is defined as previously described by Pfleger et al [29]. The cells co-transfected with KOR-Rluc and mOX2αR-Venus were used as a negative control. BRET saturation curves were obtained by transiently transfecting constant or increasing amounts of plasmids encoding the Rluc-tagged donor constructs and the Venus-tagged constructs, respectively. The total amount of plasmid DNA was kept constant by adding empty plasmid.

2.6. Fluorescence resonance energy transfer (FRET) assays

To further study the heterodimerization of APJ and B2R, FRET was carried out in living cells. The donor plasmid APJ-CFP and the receptor plasmid B2R-mVenus were co-transfected into HEK293 cells for FRET assays. HEK293 cells transfected with KOR-CFP and mOX2αR-Venus were used as a negative control. FRET signals were detected using FLUOstar OPTIMA (BMG Labtech, Offenburg, Germany) and MetaFluor 7.0 software, which allowed the sequential integration of light signals

detected with two filter settings (CFP: excitation at 436 ± 10 nm and emission at 480 ± 20 nm; mVenus: excitation at 480 ± 20 nm and emission at 535 ± 15 nm; FRET: excitation at 436 ± 10 nm and emission at 535 ± 15 nm). The equation: FRETc =FRET-(coefficient B $\times$ CFP)-(coefficient A $\times$ Venus) was used to calculate corrected FRET. Here, FRET, CFP and mVenus values correspond to background-corrected images obtained from their respective channels. Coefficient B and coefficient A correspond to the values obtained for the CFP and Venus bleed-through co-efficient, respectively, which were calculated using cells transfected with CFP and Venus individually [30, 31]. Normalized FRET ($FRET_N$) was calculated using the equation: $FRET_N$ = FRETc / (CFP $\times$ Venus). FRETc, CFP and Venus correspond to the fluorescence values obtained from single-transfected cells.

2.7. PLA

To study the APJ-B2R APJ-B2R proximity, the PLA was performed using Duolink detection kit as described previously [32, 33]. HEK293 cells co-transfected with APJ and B2R were grown on glass slides and fixed with 4% paraformaldehyde for 20 min. To detect APJ-B2R heteromers, slides were incubated with goat anti-APJ and rabbit anti-B2R antibodies at 4 °C overnight in a humidifying chamber. Slides were then washed and incubated with secondary anti-goat/rabbit antibodies conjugated PLA probes at 37 °C for 1 h. Slides were washed again and incubated with ligation-ligase solution, followed by incubation with amplification-polymerase solution. Slides were then mounted with a minimal volume of Duolink II mounting medium containing DAPI for 30 min. PLA signals were detected at room temperature under a Leika SP8 confocal microscope equipped with oil immersion objective ($\times 63$).

2.8. Co-immunoprecipitation (Co-IP)

Cells were lysed in 1% RIPA lysis buffer (Beyotime, Jiangsu, China) containing protease inhibitor cocktail (Sigma). Cell lysates containing 2 mg of protein were incubated with the anti-APJ (Thermofisher , PA5-80343) or anti-B2R (Huabio, ET7106-74) antibody protein A/G agarose complex overnight at 4℃, after mounting on a slowly rotating wheel. The beads were washed three times with with TBST and once with $4\times$ SDS-PAGE sample buffer. Equal amounts of proteins were resolved by 10% SDS–PAGE and subjected to western blotting. Detection of proteins by immunoblotting with anti-B2R (Affinity, DF8337) and anti-APJ(Bioss, bs-2430R) antibodies was conducted using an ECL system (Beyotime).

2.9. Western blotting

HUVECs and HEK293 cells were harvested in RIPA lysis buffer and the proteins concentration was measured using a bicinchoninic acid (BCA) Analysis Kit (KeyGEN, Nanjing, China). Equal aliquots of protein samples were separated on 10% SDS-PAGE gels and subsequently electrotransfered to PVDF membranes (Amersham Biosciences). The membranes were blocked with 5% lipid-free milk at room temperature for 1 h, followed by incubation with a primary antibody against B2R, APJ, or GAPDH in TBST at 4 °C overnight. After washing with TBST for 10 min $\times$ 3

times, the membrane was exposed to a HRP-conjugated secondary antibody (1:5000) at room temperature for 1 h and washed three times for 10 min/time with TBST. The immunoreactive proteins were visualized by ECL chemiluminescent reagent. Anti-GAPDH antibody was used as a loading control.

To assay eNOS and ERK1/2 activation, HUVECs endogenously expressing APJ and B2R were made quiescent by serum starvation for 24 hours prior to treatment with apelin-13 or BK. Following treatment, cells were harvested in RIPA lysis buffer. Subsequently, 10 μg of cell extracts was separated by 10% SDS-PAGE. Gel transfer was performed at 150 mA for ~90 min. Phosphorylation of eNOS and ERK1/2 were detected by immunoblotting with an antibody anti-phospho-eNOS (Ser1177(C9C3) Rabbit mAb) (Cell Signaling, USA) or anti-phospho-ERK1/2 antibody (Cell Signaling Technology) (1:2000). As a loading control, the same membranes were re-probed with an anti-total eNOS (eNOS (6H2) Mouse mAb) (Cell Signaling, USA) or anti-total ERK1/2 antibody (Cell Signaling Technology) (1:2000). The band intensities were measured by densitometric analysis, and the change in eNOS and ERK1/2 phosphorylation was calculated as the phospho-eNOS/eNOS and phospho-ERK1/2/ERK1/2 ratio, respectively.

For RNAi experiments, HUVEC cells were transiently transfected with either APJ shRNA (Sigma; clone ID: NM_004041.3-828s21c1) or B2R shRNA (Genechem; clone ID: NM_000623), and shRNA negative control (CTRL) , according to the manufacturer's instructions using Lipofectamine 2000 reagent as previously described [32]. After 48 h, the cells were collected for eNOS assays, with or without incubation with apelin-13 or BK for the indicated time periods. For U0126 and U73122 experiments, HUVECs were pretreated with ERK1/2 inhibitor U0126 (10 μM) for 1 h or phospholipase C (PLC) inhibitor U73122 (10 μM,) for 30 min, followed by stimulation with apelin-13 or BK (10^{-7} M) for 10 min.

2.10. Cell cycle analysis

For determining the cell cycle arrest properties, HUVECs were seeded in 6-well plates at a density of 1×10^5 cells/well. After 24 h, HUVECs were transfected with shRNA-APJ or shRNA-B2R plasmids. To confirm that the shRNA for B2R or APJ has no off-target effects on APJ or B2R, the APJ inhibitor F13A (1μM, 30 min) or B2R inhibitor HOE140 (10 μM, 30 min) was used prior to their agonists. After 48 h, all cells were treated with apelin-13 or BK (10^{-7} M) for 48 h. Then, cells were harvested by centrifugation and were incubated with propidium iodide (PI) using flow cytometric kits (EXBIO, Vestec, Czech Republic) according to the manufacturer's recommendations [34]. In brief, the cell plates were dissolved in a mixture of PBS and RNase A solution and incubated for 30 min. Then 1 mL of the Tris buffer solution was blended with 100 mL of PI solution and added to each cell sample. Ultimately, after 30 min incubation time in the dark at room temperature, the cell cycle analysis was carried out by a flow cytometry cytometer (Becton-Dickinson, USA).

2.11. Statistical analysis

All the data are expressed as the mean ± SEM and were presented and analyzed

using GraphPad Prism 8.0. The number of samples (n) in each experiment is provided in the figure legends. Statistical analysis was performed using an unpaired Student's t-test or a One Way ANOVA for more than two treatment conditions followed by Tukey's test. Values of $P<0.05$ were considered as statistically significant. All experiments were repeated at least three times, and representative images are shown in the figures.

3. Results

3.1. Co-expression and Co-localization of APJ and B2R in HEK293-APJ/B2R cells and HUVECs

Total proteins of HUVECs were identified for Western blot, which demonstrated that there were 43 kDa (APJ) protein band and 45 kDa (B2R) protein band (Figure 1A), suggesting both the APJ and B2R express in HUVECs. However, neither of the receptors was detected in HEK293 cells. To identify the co-localization of APJ and B2R in HEK293 cells cotransfected with pcDNA3.1-B2R and N-terminal EGFP-tagged APJ, immunofluorescence image analysis was carried out using confocal microscopy. APJ and B2R were predominantly expressed at the cell membrane (Figure 1B), implying that they may interact. Cell nuclei were visualized by DAPI staining.

To examine cell surface expression of APJ and B2R, ELISA assay was also carried out by using anti-HA and anti-Myc antibodies, respectively. Two fusion proteins HA-APJ and Myc-B2R that were N-terminally epitope-tagged with HA or Myc tags were detected. After co-expression in HEK293 cells, it was found that the cell surface expression of HA-APJ or Myc-B2R was not increased in APJ/B2R heterodimer (Figure 1C). The result from Figure 1C showed that the expression level of APJ and B2R did not change by co-expression.

3.2. APJ physically interacts with B2R

Using a variety of approaches, we examined if the functional interaction between APJ and B2R was the consequence of physical heteromerization between the two receptors. First, We carried out BRET experiments that allows the detection of energy transfer between one receptor bearing the BRET donor (Renilla luciferase) and the second receptor bearing the acceptor (green fluorescent protein) when the two receptors are in close proximity (<50Å) [35]. Under these conditions, we observed a highly significant BRET signal in cells coexpressing tagged APJ and B2R (Figure 2A). No significant BRET signal was observed in cells coexpressing KOR-Rluc and mOX2αR-Venus or co-transfected with Rluc and B2R-Venus, Venus and APJ-Rluc. The findings were supported by the demonstration of these complexes in cellular models using a BRET saturation assay. A saturable and strong BRET signal was found in the HEK293 cells cotransfected with APJ-Rluc and B2R-Venus (Figure 2B). BRET signaling demonstrated a hyperbolic function in response to increasing amounts of transfected B2R-Venus, reaching saturation at the highest concentrations obtained, whereas the negative controls with coexpressing KOR-Rluc and mOX2αR-Venus receptors [36] only produced a nonspecific linear curves (Figure 2B). The specificity

was further supported by the observation that pcDNA3.1 vector unlike wild APJ and B2R failed to compete with the formation of the APJ-B2R complex, as seen from a nonreduced BRET ratio in competition experiments (Figure 2C). Accordingly, receptor heteromers were also visualized as red spots by using PLA in cells expressing APJ and B2R but not in cells expressing KOR and mOX2αR (Figure 2D).

FRET was performed to further explore the interaction between APJ and B2R. HEK293 cells were transfected with APJ-CFP (a), B2R-Venus (b), KOR-CFP and mOX2αR-Venus (c), or APJ-CFP and B2R-Venus (d) (Figure 3A). In images of FRET, the site of interaction will be marked as yellow or red. Moreover, a more intense color means a stronger interaction. There was no significant FRET in all single-transfected cells (Figure 3, A and B). As a negative control, no significant FRET was visualized in cells cotransfected with KOR-CFP and mOX2αR-Venus. However, a notable FRET signal was clearly detected in HEK293 cells co-transfected with APJ-CFP and B2R-Venus. To verify the above results, Co-IP was used to investigate the possibility of APJ-B2R interactions in HUVECs. From Figure 3C, we can find that in the HUVECs coexpressing both APJ and B2R, APJ (or B2R) could be found in sedimentation precipitated with anti-B2R (or anti-APJ) antibody (Figure 3C). Thus, Co-IP assay indicated that APJ and B2R constitute a complex.

3.3. Apelin-13 or BK increases eNOS phosphorylation in HUVECs via APJ-B2R dimers

To determine whether APJ/B2R dimer formation affected the cellular signal transduction, time- and dose-dependent eNOS phosphorylation were investigated in HUVECs. The ability of APJ-B2R dimers to stimulate phosphorylation of eNOS was assessed by treating cells with apelin-13 or BK (10^{-7} M) for 0-60 min. As shown in Figure 3, apelin-13 significantly enhanced activation of eNOS, with maximal increase at 10 min and a return to near basal conditions after 60 min (Figure 4, A and C). In next experiments, stimulation of HUVECs with apelin-13 or BK led to a dose-dependent increase in P1177-eNOS levels (Figure 4, B and D). The results showed that apelin-13 and BK induced the time- and dose-dependent variations of eNOS phosphorylation via APJ-B2R heterodimers.

3.4. Knockdown of APJ or B2R in HUVECs affects APJ/B2R-mediated eNOS phosphorylation

To critically evaluate the role of APJ/B2R heterodimer-mediated signalling, we transfected shRNA-APJ or shRNA-B2R into HUVECs endogenously expressing both APJ and B2R receptors to observe the physiological relevance and the effects of the two receptors on eNOS phosphorylation. Western blot analyses showed that APJ and B2R were expressed in HUVECs, but treatment with shRNA-APJ or shRNA- B2R significantly decreased the expression of APJ or B2R protein (Figure 5, A and B). To investigate the effects of shRNA for APJ or B2R on B2R or APJ expression, RNAi experiments were further conducted. As shown in Figure 5A and B, shRNA for APJ reduced the B2R expression and vice versa.

In APJ knocked-down cells, in addition to apelin-13, BK treatment also decreased

eNOS phosphorylation compared to HUVECs transfected with negative control shRNA-APJ ($P<0.01$, Figure 5, C and E). Likewise, B2R depletion also reduced the apelin-13 or BK induced eNOS phosphorylation by 50-60% (Figure 5, D and F). These results suggests that the response of eNOS phosphorylation to apelin-13 or BK is mediated by the APJ-B2R heteromers.

3.5. APJ-B2R dimer induces eNOS phosphorylation via ERK1/2 signaling

Our previous study demonstrated that APJ/NTSR1 dimer induced phosphorylation of ERK1/2 and cell proliferation via Gaq-mediated mechanism [11]. To examine whether APJ-B2R dimer affects the ERK1/2 phosphorylation, dose-dependent effects of Apelin-13 and BK on ERK1/2 activation were then determined. It can be seen from the Figure 6A and C that the ERK1/2 phosphorylation increased gradually with the increase of the concentration of apelin-13 and BK, reaching the maximum at 10^{-7} M. To determine whether the phosphorylation of ERK1/2 was mediated by APJ-B2R dimers, the shRNA-APJ or shRNA-B2R was applied. As shown in Figure 6B and D-E, the results indicate that the phosphorylation of ERK1/2 reduced after APJ or B2R silenced compared to the control groups. As ERK1/2 could phosphorylate eNOS protein, we tend to ask whether the two factors interact in HUVECs under APJ-B2R dimers condition. Then HUVECs were pretreated with ERK1/2 inhibitor U0126 to inhibit ERK1/2 activation for 1 h prior to apelin-13 or BK. As shown in Figure 6F and G, p-ERK1/2 level was elevated by apelin-13 or BK action, and U0126 treatment greatly reduced this augmentation. Interestingly, the p-eNOS levels also reduced in the presence of U0126, which was consistent with the change trend of p-ERK1/2.

To examine whether eNOS phosphorylation is PLC-dependent in HUVECs, the cells were treated with the PLC inhibitor U73122 prior to apelin-13 or BK. The level of eNOS phosphorylation in HUVECs was significantly lower with U73122 treatment than without U73122 treatment (Figure 6, H and I). Furthermore, after the shRNA-APJ or shRNA-B2R was applied, the phosphorylation of eNOS significantly reduced compared to the control groups, showing that APJ and B2R are used as a complex to trigger PLC signal pathway. Collectively, these results strongly suggested that APJ-B2R dimer not only enhanced eNOS phosphorylation but also activated this protein via PLC-ERK1/2 pathway.

3.6. APJ-B2R dimers promote the cell cycle at the S phase

We investigated whether APJ-B2R dimers influences the arrest of the cell cycle in HUVECs. For this purpose, HUVECs were transfected with shRNA-APJ or shRNA-B2R plasmids, then were treated with apelin-13 or BK for 48 h and subjected to flow cytometry. As Figure 7 shows, in the HUVECs cell line, compared with those in the RNA interference group, the percentages of S phase cells increased from 16.12% to 22.92% ($P<0.01$, Figure 7A and B), 15.82% to 22.99% ($P<0.01$, Figure 7D and E), respectively. To confirm that the shRNA for B2R or APJ has no off-target effects on APJ or B2R, the APJ inhibitor F13A (10^{-7} M) or B2R inhibitor HOE140 (10 μM) was used prior to their agonists. As shown in Figure 7, when the APJ inhibitor F13A was added to the chamber for 10 min before addition of apelin, the percentages of S phase

cells significantly decreased. The similar results was found in B2R inhibitor group. These results indicate that APJ-B2R dimers significantly increase the HUVECs cell cycle at the S phase (Figure 7E). In other words, APJ-B2R dimers promotes cell proliferation after treated with apelin-13 or BK.

4. Discussion

The APJ and B2R are increasingly becoming an important subject for investigation in the cardiovascular system [37-39]. Although it has been described that both receptors are distributed in the same system and have many overlapped functions and signal pathways, the direct interaction between both receptors is not known.

In the present study, using a variety of methods such as RET assays, PLA and CO-IP, we demonstrate physical and functional interactions between APJ and B2R in recombinant as well as in HUVECs. At first, we confirmed the co-expression of APJ and B2R in HUVEC by RT-PCR and western blotting. Confocal microscopy images and ELISA showed the localization of APJ and B2R in plasma cell membrane. The identification of APJ-B2R heteromers was first carried out via biophysical technique

BRET and FRET in co-transfected HEK293 cells. The results showed that APJ

constitutively heteromerizes with B2R, but not with the unrelated receptor mOX2αR. The specificity was further supported by BRET saturation and competitive analyses, as previously described [40], so the interaction caused by molecular crowding is excluded. Several studies have reported that ligands binding may affect heterodimer formation [41, 42], whereas apelin-13 or BK treatment did not modulate the BRET ratio (data not shown).

In the FRET experiments, We labeled two receptors with CFP and mVenus, respectively, because CFP/Venus is the most popular pair of fluorescent proteins, along with its improved variant [43]. As a newly emerging technology, the PLA, which can detect nearby proteins within forty nanometers [44], has been used to identify heteromerization of μ-opioid receptors (MOR) and $α2_A$-adrenoceptors in the nucleus tractus solitarii neurons [45], and heteromerization of chemokine receptor type 4 with $α1_{A/B}$-adrenoceptors [46]. Complementary to the results of the PLA technique, data from the Co-IP experiments showed that bands corresponding to each of B2R and APJ could be detected within the eluted protein complexes, following the immunoprecipitation of HUVECs protein lysates with anti-APJ or anti-B2R. This implies that APJ and B2R could be closely associated in HUVECs. Thus, findings from the RET, PLA and co-IP experiments support the likelihood of APJ-B2R heteromerization.

Increasing studies have shown that GPCR heteromer can induced biochemical properties that are different from its individual receptors, such as ligand-binding properties, receptor-mediated G-protein activity, trafficking properties, and signal transduction [47]. For example, the CB1-D2 receptor dimers can switch CB1 from Gαi to Gαs coupling even in the absence of D2 agonist [48]. Both D1 and D2 receptors modulate the effector adenylyl cyclase, whereas D1-D2 receptor heteromer results in Gαq-mediated calcium release [49]. Our previous study also found that the

KOR and B2R can also heterodimerize to switch KOR from Gαi to Gαs coupling, leading to increase of cAMP levels [33]. B2R could constitutively interact with angiotensin Mas (1-7) receptor, resulting in unique signaling properties [50]. APJ inhibits the AT1R signalling via allosteric trans-inhibition [10]. This kind of interaction plays an important role in many biological processes. Thomas et al [51]. found that PAR4-P2Y12 heterodimer activate Akt signaling, indicating that β-arrestins play a critical role in integrin activation in vascular inflammation. Cesario et al. [52] demonstrated that low-dose CsA when combined with Cereport (selective agonist of B2R) protected nigral neurons and striatal fibers from 6-hydroxydopamine neurotoxicity, but not when given alone.

Thus, we focused on the determination of the functional characteristics of APJ-B2R receptor heteromers expressed in HUVECs. The previous reports have revealed that both APJ or B2R can signal through the eNOS pathways [53, 54]. For instance, BK promots activation of eNOS, leading to an increase of NO and subsequently leading to the regulation of vasomotor responses [55]. As a vasodilator and signaling molecule, NO plays an important physiological function including the regulation of the vascular tone, inhibition of platelet aggregation, the regulation of cell immune and so on. In addition, NO formation increased cGMP levels, reducing aortic hypertrophy and blood pressure elevation [56]. The disorders of NO biological function will causing the loss of heart protection factors, leading to the development of cardiovascular disease. Likewise, apelin-13 stimulates angiogenesis by promoting the eNOS phosphorylation in myocardial microvascular endothelial cells [57].

Therefore, we explored the implication of heteromer formation on these pathways. Finding in Figure 5 showed that APJ-B2R dimer increased the phosphorylation of eNOS in a dose- and time-dependent manner after treatment with apelin-13 or BK. However, when APJ or B2R were interfered by their respective specific shRNA, the levels of eNOS phosphorylation at Ser1177 significantly decreased after treated with apelin-13 or BK, indicating that the APJ-B2R heteromers might mediate the eNOS phosphorylation as a signaling units. In addition, both of them can reduce the expression of each other and affect the formation of dimer, which further indicates that they function as a complex. Similar phenomena occurs in other GPCR dimers. In the case of CB1R-DOR heterodimers, binding of CB1 receptor agonist or antagonist increased or inhibited the binding and consequently signaling of DOR agonist [58]. For instance, $A_{2A}R$ promoted the recruitment of β-arrestin2 to the D2R while reduced Gαi-mediated signal of the D2R in $A_{2A}R$-D2R [59]. The 5-$HT_{2A}R$-D2R heteromer did not result in altered calcium signaling, whereas the NTS1R agonist NT (8-13) decreases the Gαq-mediated Ca^{2+} signal in the NTS1R-D2R dimer [60], suggesting that the allosteric interactions can occur at GPCR heteromers to form different conformations, resulting in different binding properties [61].

As we reviewed previously, many factors including GPCR induced phosphorylation of ERK1/2 through activating Gq-PI3K-Raf or other signaling pathways [62]. Various research reported that both apelin-13/APJ and BK/B2R system could promote VSMC proliferation and angiogenesis by up-regulating activation of ERK1/2 signal pathway [63, 64]. In our present study, APJ-B2R dimer enhanced agonist-dependent

phosphorylation of ERK1/2. Interestingly, inhibiting ERK1/2 by its inhibitor U0126 significantly attenuated the activation of eNOS, suggesting that APJ-B2R dimer triggered the ERK1/2-eNOS pathway. Moreover, activation of eNOS mediated by ERK1/2 has been reported by other studies [65], where ERK1/2 increased eNOS phosphorylation in ischemic limb muscle in vivo.

In a monomeric state, B2R can be coupled with multiple G-proteins Gαq, Gαs, and Gαi, but mainly Gαq, whereas APJ mainly activate Gαi and partially Gαq. Several receptor pairs have been reported that cross-talk between Gαi- and Gαq-coupled receptors typically leads to a potentiation of Gαq coupling [66, 67]. Thus, we propose that activation of ERK1/2-eNOS mediated by APJ-B2R dimer is primarily regulated by activation of the Gαq subunit. Here, the surprising ability of U73122 to block eNOS phosphorylation indicates that APJ-B2R heteromer triggered the PLC pathway, which was usually induced by Gαq proteins. This is in agreement with our previous study of the formation between APJ and NTSR1 heterodimer, where Gαq is preferentially activated. Many studies exploring the role of GPCR heteromers in vascular remodeling and cell growth [68, 69]. The roles of APJ-B2R interaction in HUVECs proliferation (Figure 7) further suggests that the receptor dimer could represent a novel drug target for cardiovascular disease.

Taken together, we demonstrated for the first time the proximity and interaction between APJ and B2R in HUVECs and co-transfected HEK293 cells that was constitutive with possible implications on downstream PLC-ERK1/2-eNOS signaling, promoting cell proliferation. However, more insights are required for revealing the molecular mechanism of the heterodimer to provide new potential drug targets for cardiovascular disease. It is very important to search receptor-heteromer selective compounds or reagents (monovalent antibodies or membrane permeant peptides) for the treatment of a variety of physiologic disorders. Preclinical data suggest that A_{2A}–D2R receptor antagonist SCH-442416 could be useful in the treatment of drug addiction [70]. Thus, the further study is to reveal the critical interface and amino acids of APJ and B2R to screen receptor-heteromer selective drugs.

Disclosure statement

The authors declare that they have no conflicts of interest with the contents of this article.

Author contributions

Bingyuan Ji, Liyan Shang, Chunmei Wang and Lei Wan performed the experiments; Baohua Cheng analyzed the data; Bingyuan Ji wrote the manuscript; Jing Chen designed the experiments and revised the manuscript. All authors reviewed the results and approved the final version of the manuscript.

Acknowledgments

Credit author statement

Bingyuan Ji: Conceptualization, Methodology, Writing- Original draft preparation. **Liyan Shang**: Visualization, Investigation. **Lei Wan:** Software, Data curation. *Chunmei Wang*: Supervision. **Baohua Cheng**: Editing, Validation. **Jing Chen:** Writing- Reviewing.

References

[1] D. Keri, P. Barth, Reprogramming G protein coupled receptor structure and function, Curr Opin Struct Biol 51 (2018) 187-194.

[2] A.S. Hauser, M.M. Attwood, M. Rask-Andersen, H.B. Schiou, D.E. Gloriam, Trends in GPCR drug discovery: new agents, targets and indications, Nat Rev Drug Discov 16(12) (2017) 829-842.

[3] S. Ferré, V. Casadó, L.A. Devi, M. Filizola, R. Jockers, M.J. Lohse, G. Milligan, J.-P. Pin, X. Guitart, G protein-coupled receptor oligomerization revisited: functional and pharmacological perspectives, Pharmacological reviews 66(2) (2014) 413-434.

[4] K. Siddiquee, J. Hampton, D. McAnally, L. May, L. Smith, The apelin receptor inhibits the angiotensin II type 1 receptor via allosteric trans-inhibition, Br J Pharmacol 168(5) (2013) 1104-1117.

[5] O.K. Dagher, M.A. Jaffa, A. Habib, F.N. Ziyadeh, A.A. Jaffa, Heteromerization fingerprints between bradykinin B2 and thromboxane TP receptors in native cells, PLoS One 14(5) (2019) e0216908-e0216908.

[6] F. Schinzari, A. Veneziani, N. Mores, A. Barini, N. Di Daniele, C. Cardillo, M. Tesauro, Beneficial Effects of Apelin on Vascular Function in Patients With Central Obesity, Hypertension 69(5) (2017) 942-949.

[7] P. Yang, J.J. Maguire, A.P. Davenport, Apelin, Elabela/Toddler, and biased agonists as novel therapeutic agents in the cardiovascular system, Trends Pharmacol Sci 36(9) (2015) 560-567.

[8] D. C, C. H, Y. N, F. Y, H. AJ, Apela Regulates Fluid Homeostasis by Binding to the APJ Receptor to Activate Gi Signaling, The Journal of biological chemistry 290(30) (2015) 18261-8.

[9] L. Y, C. J, B. B, D. H, L. Y, L. H, Heterodimerization of human apelin and kappa opioid receptors: roles in signal transduction, Cellular signalling 24(5) (2012) 991-1001.

[10] S. K, H. J, M. D, M. L, S. L, The apelin receptor inhibits the angiotensin II type 1 receptor via allosteric trans-inhibition, Br J Pharmacol 168(5) (2013) 1104-17.

[11] B. Bai, X. Cai, Y. Jiang, E. Karteris, J. Chen, Heterodimerization of apelin receptor and neurotensin receptor 1 induces phosphorylation of ERK(1/2) and cell proliferation via Gαq-mediated mechanism, J Cell Mol Med 18(10) (2014) 2071-2081.

[12] W. L, X. F, L. C, J. B, Z. R, W. P, W. F, P. Y, Y. C, W. C, C. J, Transmembrane peptide 4 and 5 of APJ are essential for its heterodimerization with OX1R, Biochemical and biophysical research communications 521(2) (2020) 408-413.

[13] F. Marceau, J.F. Hess, D.R. Bachvarov, The B1 receptors for kinins, Pharmacological reviews 50(3)

(1998) 357-386.

[14] R. Trabold, C. Erös, K. Zweckberger, J. Relton, H. Beck, J. Nussberger, W. Müller-Esterl, M. Bader, E. Whalley, N. Plesnila, The role of bradykinin B(1) and B(2) receptors for secondary brain damage after traumatic brain injury in mice, J Cereb Blood Flow Metab 30(1) (2010) 130-139.

[15] E.-D. SS, D. S, B. WH, Bradykinin stimulates the ERK-->Elk-1-->Fos/AP-1 pathway in mesangial cells, The American journal of physiology 275(3) (1998) F343-52.

[16] Y. CM, L. MI, H. HL, S. CC, M. YH, H. LD, Bradykinin-induced p42/p44 MAPK phosphorylation and cell proliferation via Src, EGF receptors, and PI3-K/Akt in vascular smooth muscle cells, Journal of cellular physiology 203(3) (2005) 538-46.

[17] N.-S. A, P. A, P. M, T. M, K. A, G.-L. I, Bradykinin B2 and dopamine D2 receptors form a functional dimer, Biochimica et biophysica acta. Molecular cell research 1864(10) (2017) 1855-1866.

[18] W. PC, L. MH, A. KM, E.-S. HM, M. TA, P. YK, L. LM, J. AA, The arrestin-selective angiotensin AT1 receptor agonist [Sar1,Ile4,Ile8]-AngII negatively regulates bradykinin B2 receptor signaling via AT1-B2 receptor heterodimers, The Journal of biological chemistry 288(26) (2013) 18872-84.

[19] A. PM, P. A, C. RM, S. HM, Angiotensin II type 2 receptor-bradykinin B2 receptor functional heterodimerization, Hypertension 48(2) (2006) 316-22.

[20] S. Yashima, A. Shimazaki, J. Mitoma, T. Nakagawa, M. Abe, H. Yamada, H. Higashi, Close association of B2 bradykinin receptors with P2Y2 ATP receptors, J Biochem 158(2) (2015) 155-163.

[21] J. B, L. H, Z. R, J. Y, W. C, L. S, C. J, B. B, Novel signaling of dynorphin at κ-opioid receptor/bradykinin B2 receptor heterodimers, Cellular signalling 31 (2017) 66-78.

[22] A. Y, F. M, I. A, R. M, Z. A, M. MB, R. T, M. M, Post-infarct treatment with [Pyr(1)]apelin-13 improves myocardial function by increasing neovascularization and overexpression of angiogenic growth factors in rats, European journal of pharmacology 761 (2015) 101-8.

[23] K.E. Loke, C.M. Curran, E.J. Messina, S.X. Laycock, E.G. Shesely, O.A. Carretero, T.H. Hintze, Role of nitric oxide in the control of cardiac oxygen consumption in B(2)-kinin receptor knockout mice, Hypertension 34(4 Pt 1) (1999) 563-567.

[24] L. Han, J. Li, Y. Chen, M. Zhang, L. Qian, Y. Chen, Z. Wu, Y. Xu, J. Li, Human Urinary Kallidinogenase Promotes Angiogenesis and Cerebral Perfusion in Experimental Stroke, PloS one 10(7) (2015) e0134543.

[25] K. X, Q. X, L. B, W. Z, C. Y, L. X, W. W, C. SL, Modulation of low shear stress‐induced eNOS multi‐site phosphorylation and nitric oxide production via protein kinase and ERK1/2 signaling, Molecular medicine reports 15(2) (2017) 908-914.

[26] R. X, R. L, W. Q, S. H, C. L, L. N, Advanced glycation end-products decreases expression of endothelial nitric oxide synthase through oxidative stress in human coronary artery endothelial cells, Cardiovascular diabetology 16(1) (2017) 52.

[27] Q. Xue, B. Bai, B. Ji, X. Chen, C. Wang, P. Wang, C. Yang, R. Zhang, Y. Jiang, Y. Pan, B. Cheng, J. Chen, Ghrelin Through GHSR1a and OX1R Heterodimers Reveals a Gαs-cAMP-cAMP Response Element Binding Protein Signaling Pathway in Vitro, Frontiers in molecular neuroscience 11 (2018) 245-245.

[28] M.J. Orsini, J.L. Parent, S.J. Mundell, A. Marchese, J.L. Benovic, Trafficking of the HIV coreceptor CXCR4. Role of arrestins and identification of residues in the c-terminal tail that mediate receptor internalization, The Journal of biological chemistry 274(43) (1999) 31076-31086.

[29] P. KD, S. RM, E. KA, Bioluminescence resonance energy transfer (BRET) for the real-time detection of protein-protein interactions, Nature protocols 1(1) (2006) 337-45.

[30] M.J. Lohse, S. Nuber, C. Hoffmann, Fluorescence/bioluminescence resonance energy transfer

techniques to study G-protein-coupled receptor activation and signaling, Pharmacological reviews 64(2) (2012) 299-336.

[31] M.A. Ayoub, Resonance Energy Transfer-Based Approaches to Study GPCRs, Methods Cell Biol 132 (2016) 255-292.

[32] L. H, T. Y, J. B, L. H, X. Q, J. Y, D. L, Z. J, C. J, B. B, Heterodimerization of the kappa opioid receptor and neurotensin receptor 1 contributes to a novel β-arrestin-2-biased pathway, Biochimica et biophysica acta 1863(11) (2016) 2719-2738.

[33] J. B, L. H, Z. R, J. Y, W. C, L. S, C. J, B. B, Novel signaling of dynorphin at κ-opioid receptor/bradykinin B2 receptor heterodimers, Cellular signalling 31(undefined) (2017) 66-78.

[34] H. K, S. MH, M. B, D. MA, V. F, A. M, M. A, S. D, B. B, Alpha7 Nicotinic Acetylcholine Receptor Mediates Nicotine-induced Apoptosis and Cell Cycle Arrest of Hepatocellular Carcinoma HepG2 Cells, Advanced pharmaceutical bulletin 10(1) (2020) 65-71.

[35] A. S, S. A, J. E, H. S, C. D, D. M, B. M, Detection of beta 2-adrenergic receptor dimerization in living cells using bioluminescence resonance energy transfer (BRET), Proceedings of the National Academy of Sciences of the United States of America 97(7) (2000) 3684-9.

[36] C. Wang, Y. Pan, R. Zhang, B. Bai, J. Chen, H.S. Randeva, Heterodimerization of mouse orexin type 2 receptor variants and the effects on signal transduction, Biochimica et biophysica acta 1843(3) (2014) 652-63.

[37] C. Read, D. Nyimanu, T.L. Williams, D.J. Huggins, P. Sulentic, R.G.C. Macrae, P. Yang, R.C. Glen, J.J. Maguire, A.P. Davenport, International Union of Basic and Clinical Pharmacology. CVII. Structure and Pharmacology of the Apelin Receptor with a Recommendation that Elabela/Toddler Is a Second Endogenous Peptide Ligand, Pharmacological reviews 71(4) (2019) 467-502.

[38] A. Siltari, R. Korpela, H. Vapaatalo, Bradykinin-induced vasodilatation: Role of age, ACE1-inhibitory peptide, mas- and bradykinin receptors, Peptides 85 (2016) 46-55.

[39] J.-C. Zhong, Z.-Z. Zhang, W. Wang S.M... McKinnie, J.C. Vederas, G.Y. Oudit, Targeting the apelin pathway as a novel therapeutic approach for cardiovascular diseases, Biochim Biophys Acta Mol Basis Dis 1863(8) (2017) 1942-1950.

[40] D.O. Borroto-Escuela, X. Li, A.O. Tarakanov, D. Savelli, M. Narváez, K. Shumilov, Y. Andrade-Talavera, A. Jimenez-Beristain, B. Pomierny, Z. Díaz-Cabiale, R. Cuppini, P. Ambrogini, M. Lindskog, K. Fuxe, Existence of Brain 5-HT1A-5-HT2A Isoreceptor Complexes with Antagonistic Allosteric Receptor-Receptor Interactions Regulating 5-HT1A Receptor Recognition, ACS Omega 2(8) (2017) 4779-4789.

[41] N.A. Balenga, E. Martínez-Pinilla, J. Kargl, R. Schröder, M. Peinhaupt, W. Platzer, Z. Bálint, M. Zamarbide, I.G. Dopeso-Reyes, A. Ricobaraza, J.M. Pérez-Ortiz, E. Kostenis, M. Waldhoer, A. Heinemann, R. Franco, Heteromerization of GPR55 and cannabinoid CB2 receptors modulates signalling, Br J Pharmacol 171(23) (2014) 5387-5406.

[42] M. Bellot, S. Galandrin, C. Boularan, H.J. Matthies, F. Despas, C. Denis, J. Javitch, S. Mazères, S.J. Sanni, V. Pons, M.-H. Seguelas, J.L. Hansen, A. Pathak, A. Galli, J.-M. Sénard, C. Galés, Dual agonist occupancy of AT1-R-α2C-AR heterodimers results in atypical Gs-PKA signaling, Nature chemical biology 11(4) (2015) 271-279.

[43] L. MJ, N. S, H. C, Fluorescence/bioluminescence resonance energy transfer techniques to study G-protein-coupled receptor activation and signaling, Pharmacological reviews 64(2) (2012) 299-336.

[44] K.-J. Leuchowius, I. Weibrecht, U. Landegren, L. Gedda, O. Söderberg, Flow cytometric in situ proximity ligation analyses of protein interactions and post-translational modification of the epidermal

growth factor receptor family, Cytometry A 75(10) (2009) 833-839.

[45] G.-C. Sun, W.-Y. Ho, B.-R. Chen, P.-W. Cheng, W.-H. Cheng, M.-C. Hsu, T.-C. Yeh, M. Hsiao, P.-J. Lu, C.-J. Tseng, GPCR dimerization in brainstem nuclei contributes to the development of hypertension, Br J Pharmacol 172(10) (2015) 2507-2518.

[46] A.E. Evans, A. Tripathi, H.M. LaPorte, L.I. Brueggemann, A.K. Singh, L.J. Albee, K.L. Byron, N.I. Tarasova, B.F. Volkman, T.Y. Cho, V. Gaponenko, M. Majetschak, New Insights into Mechanisms and Functions of Chemokine (C-X-C Motif) Receptor 4 Heteromerization in Vascular Smooth Muscle, International journal of molecular sciences 17(5) (2016) 971.

[47] S. Ferré, R. Baler, M. Bouvier, M.G. Caron, L.A. Devi, T. Durroux, K. Fuxe, S.R. George, J.A. Javitch, M.J. Lohse, K. Mackie, G. Milligan, K.D.G. Pfleger, J.-P. Pin, N.D. Volkow, M. Waldhoer, A.S. Woods, R. Franco, Building a new conceptual framework for receptor heteromers, Nature chemical biology 5(3) (2009) 131-134.

[48] K. CS, B.-P. K, D. E, M. K, G. M, Concurrent stimulation of cannabinoid CB1 and dopamine D2 receptors enhances heterodimer formation: a mechanism for receptor cross-talk?, Molecular pharmacology 67(5) (2005) 1697-704.

[49] H. A, F. T, A. M, N. T, P. ML, O.D. BF, G. SR, Calcium signaling cascade links dopamine D1-D2 receptor heteromer to striatal BDNF production and neuronal growth, Proceedings of the National Academy of Sciences of the United States of America 106(50) (2009) 21377-82.

[50] B.D. Cerrato, O.A. Carretero, B. Janic, H.E. Grecco, M.M. Gironacci, Heteromerization Between the Bradykinin B2 Receptor and the Angiotensin-(1-7) Mas Receptor: Functional Consequences, Hypertension 68(4) (2016) 1039-1048.

[51] T.H. Smith, J.G. Li, M.R. Dores, J. Trejo, Protease-activated receptor-4 and purinergic receptor P2Y12 dimerize, co-internalize, and activate Akt signaling via endosomal recruitment of beta-arrestin, The Journal of biological chemistry 292(35) (2017) 13867-13878.

[52] C.V. Borlongan, D.F. Emerich, B.J. Hoffer, R.T. Bartus, Bradykinin receptor agonist facilitates low-dose cyclosporine-A protection against 6-hydroxydopamine neurotoxicity, Brain research 956(2) (2002) 211-20.

[53] S. MM, R. NM, A.D. BA, R. MA, A.E.E. A, Protective effect of apelin preconditioning in a rat model of hepatic ischemia reperfusion injury; possible interaction between the apelin/APJ system, Ang II/AT1R system and eNOS, United European gastroenterology journal 7(5) (2019) 689-698.

[54] S. JB, Role of Bradykinin in the Regulation of Endothelial Nitric Oxide Synthase Expression by Cardiovascular Drugs, Current pharmaceutical design 23(40) (2017) 6215-6222.

[55] D. Thuringer, L. Maulon, C. Frelin, Rapid transactivation of the vascular endothelial growth factor receptor KDR/Flk-1 by the bradykinin B2 receptor contributes to endothelial nitric-oxide synthase activation in cardiac capillary endothelial cells, The Journal of biological chemistry 277(3) (2002) 2028-32.

[56] J.J. Zhang, L. Chao, J. Chao, Adenovirus-mediated kallikrein gene delivery reduces aortic thickening and stroke-induced death rate in Dahl salt-sensitive rats, Stroke 30(9) (1999) 1925-31; discussion 1931-2.

[57] Y. X, Z. W, Z. P, C. K, Z. L, L. J, W. M, L. M, Apelin-13 stimulates angiogenesis by promoting cross‑talk between AMP-activated protein kinase and Akt signaling in myocardial microvascular endothelial cells, Molecular medicine reports 9(5) (2014) 1590-6.

[58] S. S, G. A, G. I, F. M, R. A, B. EN, D. LA, Targeting Cannabinoid 1 and Delta Opioid Receptor Heteromers Alleviates Chemotherapy-Induced Neuropathic Pain, ACS pharmacology & translational

science 2(4) (2019) 219-229.

[59] F. K, B.-E. DO, T. AO, R.-F. W, F. L, T. S, P.-A. M, D.P. M, A. LF, Dopamine D2 heteroreceptor complexes and their receptor-receptor interactions in ventral striatum: novel targets for antipsychotic drugs, Progress in brain research 211 (2014) 113-39.

[60] P. M, S. T, B.-E. DO, W. D, G. P, F. K, F. K, Differential allosteric modulation within dopamine DR - neurotensin NTS1R and DR - serotonin 5-HTR receptor complexes gives bias to intracellular calcium signalling, Scientific reports 9(1) (2019) 16312.

[61] G. TM, R. M, D. M, M. RU, S. S, Minute-scale persistence of a GPCR conformation state triggered by non-cognate G protein interactions primes signaling, Nature communications 10(1) (2019) 4836.

[62] K. T, L. M, J. B, B. B, C. B, W. C, Role of the Extracellular Signal-Regulated Kinase 1/2 Signaling Pathway in Ischemia-Reperfusion Injury, Front Physiol 10 (2019) 1038.

[63] L. X, L. J, Z. H, C. L, Apelin/APJ system: A critical regulator of vascular smooth muscle cell, Journal of cellular physiology 233(7) (2018) 5180-5188.

[64] H. L, L. J, C. Y, Z. M, Q. L, C. Y, W. Z, X. Y, L. J, Human Urinary Kallidinogenase Promotes Angiogenesis and Cerebral Perfusion in Experimental Stroke, PLoS One 10(7) (2015) e0134543.

[65] Q. X, O. Y, M. T, W. F, O. O, O. R, Y. K, D. W, S. N, Y. Y, T. N, T. /, Sustained delivery of sphingosine-1-phosphate using poly(lactic-co-glycolic acid)-based microparticles stimulates Akt/ERK-eNOS mediated angiogenesis and vascular maturation restoring blood flow in ischemic limbs of mice, European journal of pharmacology 634 (2010) 121-31.

[66] R. ML, V. C, F. Y, T. N, T. E, A. MA, S. R, P. JP, P. L, Crosstalk between GABAB and mGlu1a receptors reveals new insight into GPCR signal integration, The EMBO journal 28(15) (2009) 2195-208.

[67] R. R, G. A, G. K, L. MP, G. I, L.-R. D, N. N, O. L, AT1R-CB1R heteromerization reveals a new mechanism for the pathogenic properties of angiotensin II, The EMBO journal 30(12) (2011) 2350-63.

[68] K.K.V. Haack, M.R. Tougas, K.T. Jones, S.S. El-Dahr, H. Radhakrishna, N.A. McCarty, A novel bioassay for detecting GPCR heterodimerization: transactivation of beta 2 adrenergic receptor by bradykinin receptor, J Biomol Screen 15(3) (2010) 251-260.

[69] T. Aspelin, M. Eriksen, A. Ilebekk, A. Cataliotti, C.R. Carlson, T. Lyberg, β-blockade abolishes the augmented cardiac tPA release induced by transactivation of heterodimerised bradykinin receptor-2 and β2-adrenergic receptor in vivo, Thromb Haemost 112(5) (2014) 951-959.

[70] S. Ferre, V. Casado, L.A. Devi, M. Filizola, R. Jockers, M.J. Lohse, G. Milligan, J.P. Pin, X. Guitart, G protein-coupled receptor oligomerization revisited: functional and pharmacological perspectives, Pharmacol Rev 66(2) (2014) 413-34.

Figure 1. Co-expression and co-localization of APJ and B2R in HUVECs and HEK293 cells. (A) APJ (left, 43KD) and B2R (right, 45KD) expression in HUVECs and HEK293 cells were detected by western blotting. (B) Confocal microscopy analysis of the co-localization of APJ and B2R was performed in HEK293 cells after transient co-transfected with pEGFP-APJ (green) and pcDNA3.1-B2R. pcDNA3.1-B2R was immunostained with AlexaFluor 647 (red). Co-localization is showed in merged images. Nuclei appears in blue. Immunofluorescence was measured with a Leica SP8 confocal microscope. (C) Determination of cell surface expression of APJ and B2R. HA-tagged APJ and Myc-tagged B2R were transfected singly or together into HEK293 cells. ELISA was conducted with intact cells using anti-Myc and anti-HA antibodies. Data are expressed as means ± SEM of triplicate

determinations. NS, non-significant.

Figure 2. APJ-B2R dimerization assessed by BRET and PLA. (A) Heterodimerization of APJ and B2R was measured in the four indicated conditions by BRET. Twenty-four hours after transfection, the fluorescence and luminescence of each sample were measured prior to every experiment to confirm equal expression of Rluc while monitoring the increase in Venus expression. BRET ratios were analyzed and expressed as the means $\pm$ SEM of four experiments. $P<0.001$ vs. other three groups. (B) BRET saturation assay. HEK293 cells were transfected with Rluc construct and increasing amounts of the Venus construct. BRET, expressed as mBU, is given as a function of 1000 ratio of fluorescence of the acceptor (Venus) and Luciferase activity of the donor (Rluc). Data are mean$\pm$SEM, n=3. (C) BRET competition experiment for the APJ-B2R receptor complexes. A fixed ratio (1:1) of expression levels of the APJ-Rluc and B2R-Venus plasmids was used in the presence of increasing concentrations of wild-type receptors and pcDNA3.1$^+$ vector. Data were expressed as means $\pm$ SEM of six experiments. $P<0.01$, $P<0.001$ vs. pcDNA3.1$^+$ group. (D) Confocal microscopy images (superimposed sections) from PLA experiments performed in HEK-293 cells transfected with APJ cDNA and B2R cDNA (left) or KOR cDNA and mOX2αR cDNA (right). Heteromeric complexes appearaed red spots and nuclei was stained with DAPI (blue).

Figure 3. Assessment of dimerization of APJ and B2R using FRET and co-IP assays. (A) FRET imaging of constitutive APJ-B2R heteromeric interactions in living cells. HEK293 cells were transiently transfected (co-expressed or individually expressed) with the following plasmids: (a) APJ-CFP, (b) B2R-Venus, (c) KOR-CFP and mOX2αR-Venus, and (d) APJ-CFP and B2R-Venus. Left-hand panels, CFP; center panels, Venus; right-hand panels, corrected FRET. (B) Calculated normalized FRET values were assessed and shown as described in the *Materials and Methods*. $P<0.001$ vs. other groups. Data are means $\pm$ SEM of at least three independent experiments. (C) APJ-B2R interactions in HUVEC as revealed by Co-IP. HUVECs lysates were immunoprecipitated with anti-APJ followed by immunoblotting with anti-B2R (upper panels) antibodies, or immunoprecipitated with anti-B2R followed by immunoblotting with anti-APJ (lower panels), successively.

Figure 4. Activity of APJ/B2R-mediated p1177-eNOS phosphorylation in HUVECs after treated with apelin-13 or BK. (A) Time-dependent p1177-eNOS phosphorylation. HUVECs were treated with apelin-13 (10^{-7} M) or BK (10^{-7} M) for 0 min, 5 min, 10 min, 15 min, 30 min and 60 min. (B) Dose-dependent p1177-eNOS phosphorylation. HUVECs were treated with apelin-13 (10^{-11}-10^{-7} M) or BK (10^{-11}-10^{-7} M) for 10 min. The time-dependent and dose-dependent effects of the treatments were quantified (C-D). All the data represent the mean $\pm$ SEM of three measurements from three independent experiments. *$P<0.05$, ** $P<0.01$ compared to basal.

Figure 5. Knockdown of APJ or B2R in HUVECs affects APJ/B2R-mediated eNOS

phosphorylation. HUVECs were transfected with shRNA-APJ or shRNA-B2R, and the control shRNA (CTL) as the negative control. Representative APJ or B2R western blots from un-transfected, control shRNA-, or specific shRNA-transfected HUVEC are shown (A and B, upper lands). GADPH was used as the loading control. (C-F) HUVECs were transfected with shRNA-APJ, shRNA-B2R or control shRNA as previously described, and cells were treated or untreated with apelin-13 (10^{-7} M) or BK (10^{-7} M) for 10 min. Phosphor1177-eNOS (p-eNOS) expression were detected by Western blot, eNOS was used as the loading control. *$P < 0.05$, **$P < 0.01$ *vs.* control shRNA group.

Figure 6. ERK1/2-eNOS signaling induced by APJ-B2R dimers. (A) Dose-dependent ERK1/2 phosphorylation. HUVECs were treated with apelin-13 (10^{-11}-10^{-7} M) or BK (10^{-11}-10^{-7} M) for 10 min. The dose-dependent effects of the treatments were quantified (C). (B) The effects of shRNA-APJ or shRNA-B2R on the phosphorylation of ERK1/2. HUVECs transfected with shRNA-APJ or shRNA-B2R were treated with apelin-13 (10^{-7} M) or BK (10^{-7} M) for 10 min. (D-E) *$P < 0.05$ in comparison with shRNA-B2R group, **$P < 0.01$ in comparison with shRNA-APJ group. (F-G) HUVECs were pretreated with ERK1/2 inhibitor U0126 (10 μM for 1 h) followed stimulated with apelin-13 or BK (10^{-7} M) for 10 min. (H-I) HUVECs were transfected with or without receptors shRNA and then pretreated with PLC inhibitor U73122 (10 μM for 30 min) followed treated with apelin-13 or BK (10^{-7} M) for 10 min. All results are mean ± SEM of at least three independent experiments. *$P < 0.05$, **$P < 0.01$ for pairwise comparisons.

Fig.7 HUVECs cell cycle induced by apelin-13 or BK, as determined by flow cytometry. The cell cycle distribution of HUVECs was determined after treatment with apelin-13 (A), apelin plus shRNA-B2R (B), apelin plus HOE140 (C) or BK (D), BK plus shRNA-APJ (E), BK plus F13A (F). (G) Flow cytometry analysis showed that shRNA-APJ, shRNA-B2R, HOE140 or F13A inhibited cell cycle proliferation by reducing S phase arrest. Data are presented as the mean±SEM from three independent experiments, *$P < 0.05$, **$P < 0.01$.

Highlights

- APJ and B2R form heterodimers that function as a novel pharmacological entity.
- APJ/B2R heteromers mediate the PLC-ERK1/2-eNOS signaling pathway.
- Apelin-13 enhances proliferation of HUVECs.
- We reveal the molecular mechanism underlying cardiovascular protection mediated by APJ/B2R heterodimers.